Nature Environment and Pollution Technology
An International Quarterly Scientific Journal

p-ISSN: 0972-6268
(Print copies up to 2016)
e-ISSN: 2395-3454

Vol. 24 | No. 4 | Article ID B4296 | 2025

Original Research Paper

https://doi.org/10.46488/NEPT.2025.v24i04.B4296

Open Access Journal

Assessment of Soil Erosion and Sediment Yield Using GIS-Based RUSLE Modeling- A Case Study of Musi Sub-Basin, Telangana, India

Shiva Chandra Vaddiraju†
Department of Civil Engineering, Maturi Venkata Subba Rao (MVSR) Engineering College, Hyderabad, Telangana, India
†Corresponding author: Shiva Chandra Vaddiraju, shivachandra135@gmail.com

Abbreviation: Nat. Env. & Poll. Technol.
Website: www.neptjournal.com

Received: 18-12-2024
Revised: 11-02-2025
Accepted: 16-02-2025

Key Words:

Geographical Information System
Google Earth Engine
RUSLE
LULC
Musi river basin

ABSTRACT

Soil loss, also known as erosion, is an irreversible natural phenomenon that affects the topsoil of the Earth's surface. It reduces soil fertility and water availability, and initiates geo-hazards, leading to negative environmental consequences. A research study was conducted in part of the Musi River sub-basin, a tributary of the Krishna River basin in India, which is undergoing a lot of changes due to anthropogenic factors. The novelty of this study lies in the integration of the RUSLE (Revised Universal Soil Loss Equation) model with advanced Geographical Information System (GIS) techniques to evaluate soil erosion and sediment yield in the basin. Leveraging the capabilities of the Google Earth Engine platform, the study employs the CART (Classification and Regression Trees) machine learning algorithm to generate the LULC (Land Use Land Cover) map, crucial for accurate C factor estimation. This innovative approach improves the precision of erosion modeling by seamlessly integrating GIS, machine learning, and remote sensing technologies. The analysis reveals that the LULC map has a total accuracy of 89.6% and a kappa coefficient of 0.86. The analysis also shows that the agriculture class dominates the research area with 51.4%. The results reveal that 95.6% of the research area has very low soil erosion of 0-1 ton/ha/year, and 60.8% of the area has low sediment yield of 0-1 ton.ha^{-1}.y^{-1}. As the study area consists of major towns and cities, and the agricultural area is being converted to open plots (barren lands for developmental activities), erosion may increase in the future. The findings of this study may be used by managers and legislators to suggest soil conservation laws to expedite development projects.

Citation for the Paper:

Vaddiraju, S.C., 2025. Assessment of soil erosion and sediment yield using GIS-based RUSLE modeling- A case study of Musi Sub-Basin, Telangana, India. *Nature Environment and Pollution Technology*, 24(4), B4296. https://doi.org/10.46488/NEPT.2025.v24i04.B4296

Note: From 2025, the journal has adopted the use of Article IDs in citations instead of traditional consecutive page numbers. Each article is now given individual page ranges starting from page 1.

INTRODUCTION

Soil is an irreplaceable resource that cannot be replaced once it is gone. In the past, there was a lack of foresight and knowledge, whereas today, negligence and overexploitation have formed a land degradation problem having huge implications. Soil erosion not only removes the top layer of soil and vegetation but also depletes the entire layer of productive soil, which contains essential nutrients for plants, organic carbon, humus, beneficial microorganisms, and other vital components. In addition to negatively impacting the diversity of animals, plants, and microbes, it lowers soil quality, which lowers natural soil capital and the delivery of ecosystem services associated with soil. This decreases productivity in agriculture, forests, and overall ecosystems (Steinhoff-Knopp et al. 2021). Erosion impacts agriculture directly and also causes several indirect effects, including the deterioration of water quality, excessive siltation in streams, wetlands, channels, and reservoirs, which reduces their capacity to store and absorb water. This contributes to destructive floods, droughts, and significant economic and ecological consequences tied to these natural resources (Schmidt 2000, Poesen et al. 2003, Jamal et al. 2022a, Salahalden et al. 2024). Globally, both human activities and natural factors drive soil erosion and degradation, posing critical challenges for human society (Panagos et al. 2017). The expansion of wastelands because of soil erosion is causing degradation of land, which calls

into question the sustainability of the environment (Zhao et al. 2013, Dai et al. 2015, Prosdocimi et al. 2016, Behera et al. 2017, Gaonkar et al. 2024). Erosion has accelerated due to human-caused factors such as land use changes, agriculture, deforestation, urbanization, and climate change (Borrelli et al. 2020, Ganaie et al. 2020, Jamal & Ahmad 2020). Approximately 84% of global land loss is attributed to soil erosion (Opeyemi et al. 2019), with an average erosion rate ranging from 12 to 15 tonnes per hectare per year (Ashiagbor et al. 2013). Soil loss due to surface runoff poses a serious threat to vulnerable landscapes (Sahana et al. 2020). For example, Northeast China's fertile black soil region has experienced severe and worsening soil erosion over time (Liu & Liu 2020). Similarly, significant areas in Ilam province, western Iran, and Calabria, southern Italy, are heavily affected by gully erosion (Terranova et al. 2009). The rapid expansion of this issue has led to reduced agricultural productivity and water availability.

Since the 1930s, scientists have employed soil erosion hazard assessments to predict erosion and develop mitigation strategies (Renard et al. 1994, Dutta et al. 2015). Water-induced soil loss has been estimated using various techniques at local, regional, and global levels (Mesfin 1994). Numerous models have been developed to quantify soil loss rates, including physical-process-based models, semi-empirical models, and empirical models (Gayen et al. 2019, Poesen et al. 2003, Pan & Wen 2014). However, inadequate sample plots and traditional field-based methods have often led to inconsistent spatial assessments of erosion. Moreover, these methods are expensive and time-intensive, making it challenging to map and monitor soil loss distribution over large areas (Prasannakumar et al. 2011). In order to predict how much soil will erode over time (Abdo & Salloum, 2017), the US Department of Agriculture developed the USLE (Universal Soil Loss Equation) in 1978. This empirical method uses plot data gathered in the eastern US to assess the long-term means of rill along sheet erosion (Wischmeier & Smith 1965). A more recent version of USLE, known as the RUSLE, was supplied by Renard et al. (1997). Even though it's an empirical method, RS, GIS, and RUSLE work together to provide estimates of soil erosion and its geographic distribution at reasonable costs and having higher accuracy across wider areas. Because of its simple model structure and minimal data needs, the empirical equation of the RUSLE continues to be the most appropriate approach for determining the risk of soil erosion, according to the authors (Lu et al. 2004, Bahadur, 2009, Perovic et al. 2013). This is especially true for the majority of poor countries, where a deficiency of suitable input data may limit the use of more complex models (Pan & Wen 2014). As a result, the purpose of this research has been to evaluate soil loss and estimate the sediment yield in the Musi Subbasin portion utilizing GIS, RS, and the RUSLE model. Decision-makers may use this to plan for optimal soil restoration and to implement sustainable land management techniques.

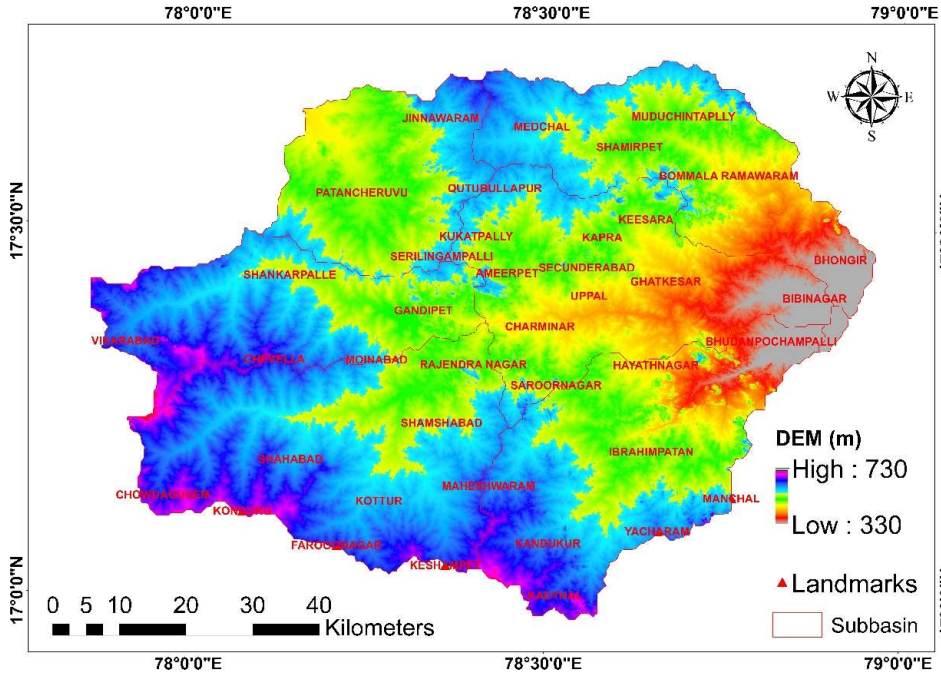

Fig. 1: Study Area Map.

STUDY AREA

The Musi basin is a part of the Krishna River basin in India. Musi River originates at Anantha Giri Hills, near Vikarabad City in the state of Telangana. Musi River flows through Hyderabad city before culminating into the Krishna River at Vadapally near Miryalaguda town in Nalgonda district. A part of the Musi subbasin covering an area of 6346 sq. km is considered in the present study. There are seven watersheds in the research region. The research area's climate is characteristic of the Deccan Plateau's semi-arid, rain-fed environment. Winters are pleasant, while summers are hot. It is subject to both the North-East and South-West monsoons. The 760 mm of yearly rainfall is scattered unevenly across space. The Musi sub-basin is selected as the present study area due to its distinct geographic, climatic, and socio-economic characteristics. It is located in a semi-arid environment and receives 760 mm of rainfall per year, with severe monsoons and long dry periods leading to soil erosion. Its varied elevation (330 meters to 730 meters) creates diverse slopes that influence runoff and erosion processes. Rapid urbanization in Hyderabad alters land use and increases runoff, while downstream rural areas face significant impacts on agriculture and water quality. Soil erosion here causes sedimentation, reduced productivity, and water degradation, directly affecting local livelihoods. Studying this region addresses critical knowledge gaps and supports effective soil and water conservation strategies. These factors make the Musi sub-basin a model for sustainable resource management. The study area map is depicted in Fig. 1.

MATERIALS AND METHODS

Estimation of Soil Erosion Rate Using the RUSLE Model

In this research, the RUSLE model was utilized to compute the yearly soil erosion. Equation 1 (Renard 1997) employed in this model is as follows:

$$A = R \times K \times LS \times C \times P \quad \ldots(1)$$

A	average annual soil loss	(ton.ha^{-1}. y^{-1})
K	soil erodibility factor	(ton.h^{-1}.MJ^{-1}.mm^{-1})
R	rainfall erosivity factor	(MJ.mm.ha^{-1}.h^{-1} .y^{-1})
P	support practice factor	(unitless)
C	cover management factor	
LS	slope length factor	

Estimation of Rainfall Erosivity Factor (R)

The capacity of rainfall to separate and move soil particles, thereby causing soil erosion, is what determines rainfall erosivity (R). R computation requires continuous and comprehensive rainfall data (Ganasari & Ramesh 2016). Calculating the R-factor is a challenging procedure that is heavily reliant on the length, volume, energy, intensity, and raindrop size, as well as on the pattern of precipitation and the rates of runoff that follow (Farhan & Nawaiseh 2015). Rainfall erosivity can be computed using the intensity of the rainfall (Amellah & Morabiti,2021). However, the lack of high-resolution rainfall data makes calculating the R-factor difficult in most of the world (Thomas et al. 2017). Annual rainfall data from 65 stations is collected from the chief planning officers of Ranga Reddy, Hyderabad, Medchal-Malkajgiri, and Nalgonda districts, and the rainfall map is prepared utilizing the Inverse Distance Weighing (IDW) approach in ArcMap 10.7. Later, the rainfall erosivity factor is calculated using Equation 2.

$$R = 79 + 0.363R_a \quad \ldots(2)$$

Where R_a represents as mean annual precipitation, and R as the erosivity factor.

Soil Erodibility Factor (K)

The ease with which particles of soil could separate from the host soil and be carried away by rainwater is measured by the soil erodibility factor (K). The organic matter content, texture, permeability, and structure of the soil all play major roles in calculating the K factor. According to Ganasri & Ramesh (2016), soil erosion is defined as the "rate of erosion per unit of the erosion index from a typical unit plot of 22.13 m in length with a slope gradient of 9%." It displays the soil loss rate divided by the rainfall erosivity (R) index. The basin's soil map was created using the FAO (Food and Agriculture Organization) Soil Map available on the Geo Network Web Portal, and the soil type and k factor are determined using the guidelines provided by Stone & Hilborn (2000).

Topography Factor (LS)

The topography's impact on erosion rate is presented by the RUSLE variables L and S. Greater slope length and steepness result in increased overland flow and soil erosion (Siswanto & Sule 2019). Moreover, changes in the slope have a much greater impact on total soil loss as compared to changes in the length of the slope (McCool et al. 1987). When the ground slope surpasses the critical angle, the topography becomes a crucial factor. When the slope of the ground is greater than the critical angle, the topography comes into play. Utilizing the SRTM DEM and Spatial Analyst toolbar in ArcMap 10.7, the flow accumulation and slope are calculated, and finally, the LS factor is determined. The Moore and Burch equation 3 is used to compute the LS factor (1986). The

Moore and Burch (1986) equation was chosen because of its empirical accuracy, simplicity, and computing efficiency when calculating the LS factor. It adapts well to different slope lengths and steepness's and is frequently used within the RUSLE framework, ensuring consistency and reliability in soil erosion modelling.

$$LS = (\text{Flow Accumulation} \quad \text{Cell size} /22.13)^{0.4} (\sin \text{slope} /0.896)^{1.3} \quad \ldots(3)$$

Land Management Factor (C)

The influence of LULC types on the rate of soil erosion is described by the C factor. Calculating the C factor requires knowledge of soil moisture, soil surface variation, crop role, and soil management. However, it is challenging to evaluate any of these features due to a lack of data and the large number of conceivable combinations (Farhan & Nawaiseh 2015). Following the recommendations of Yesuph and Dagnew (2019) and Fayas et al. (2019), we determined the C parameter for this study by using the basin's LULC map. The LULC map is prepared by using Sentinel 1 data and the CART machine learning algorithm in Google Earth Engine for the year 2023. The LULC map is prepared using Agriculture, Vegetation, Built-up, Waterbody, and Barren Land classes. The training samples taken are as follows: Agriculture-76, Vegetation-75, Builtup-75, Waterbody-65, and Barrenland-70, respectively. The accuracy of the classified LULC map is found by the confusion matrix, overall accuracy, and the kappa coefficient. We then vectorized the raster map to display the relevant C factor for every LULC category, following a method suggested by the literature (Swarnkar et al. 2018, Maqsoom et al. 2020, Allafta & Opp 2022). C factor values of 0, 0,0.5,0.6,1 are assigned to water bodies, built-up, Vegetation, Agriculture, and Barren Land.

Conservation Practice Factor (P)

The P factor calculates how much a particular site's soil loss is affected by conservation techniques like contouring, terracing, and buffer belts of closely spaced plants. By restricting the velocity and volume of runoff and encouraging the deposition of sediment on the slope surface, implementing these beneficial conservation practices lowers the P-value. The literature has numerous tables and formulae that provide P values for the various supporting conservation acts (McPhee & Smithen 1984). The P factor in this investigation was calculated using the Wener approach (Lufafa et al. 2003), which involved the use of equation 4.

$$P = 0.2+0.03S \quad \ldots(4)$$

Where S is the slope grade in percent.

Sediment Yield

Zarris et al. (2011) suggested that accurately estimating sediment yield at various scales is crucial for addressing land degradation, implementing irrigation, and generating hydropower. However, only a portion of the eroded granules reach the basin outflow, which could end up in channels or tanks. Thus, one of the most important first steps in estimating Sediment Yield is to compute the Sediment Delivery Ratio. A

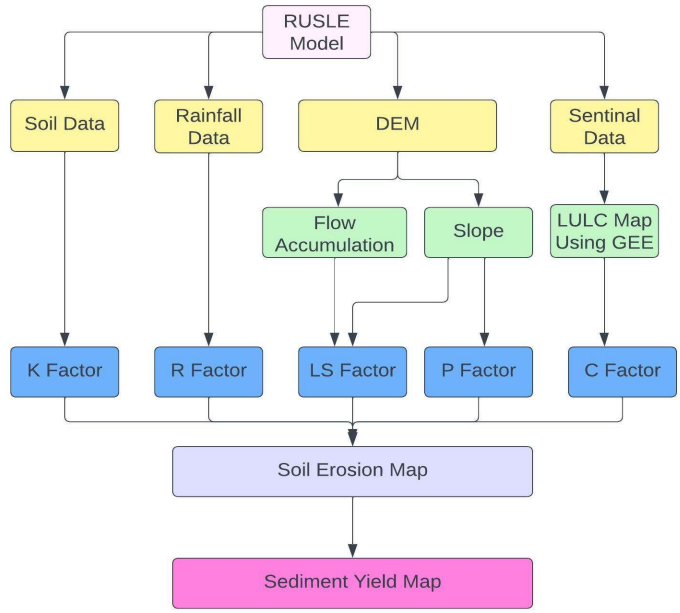

Fig. 2: Methodology adopted in the present study.

wide range of SDR models, from the most straightforward—empirical—to the most intricate—physically based—were developed and employed in several studies. As per SDR, the amount of Sediment Yield supplied to the basin's outlet is primarily influenced by catchment parameters like soil type, aspect, basin gradient, surface quality, basin extent, and channel gradient. Though the SDR has limitations like inaccuracies in heterogeneous soil types, land cover, and climate conditions, it is generally used due to its simplicity and practicality. According to Vanoni (1975), the Sediment Deposit Ratio can be calculated using Equation 5, and the sediment yield can be determined using Equation 6.

$$\text{Sediment Delivery Ratio} = 0.42\ A^{-0.125} \quad \ldots(5)$$

Where A is a basin area in sq. km.

$$\text{Sediment yield} = \text{Sediment Delivery Ratio Soil Erosion} \quad \ldots(6)$$

Fig. 2 shows the overall methods used in this investigation.

RESULTS AND DISCUSSION

R Factor

Average rainfall is a stronger predictor of seasonal variability in soil erosion rates compared to annual rainfall, which is often preferred for its reliability, simplicity, and geographic consistency (Qin et al. 2023). However, precipitation intensity is a key factor, as higher intensity increases runoff and amplifies soil erosion (Kolli et al. 2021). It is necessary to take measurements of the intensity of the rainfall to calculate the R factor, which is a measurement of the kinetic energy of the rain (Teng et al. 2019). The R factor in the current study has been determined using the average yearly rainfall. R has a value between 373.28 and 613.26 $MJ.mm^{-1}.ha^{-1}.h.y^{-1}$. The R Factor has more value in Medchal and Bongir mandals. The erosivity map of the rain, created using the study area's rainfall data, is displayed in Fig. 3.

K Factor

The k factor is a value that measures soil's natural resistance to particle detachment and transport during precipitation (Thomas et al. 2017, Kebede et al. 2021). Researchers have developed a wide range of ways for determining soil erodibility. The most common way is to employ the soil erodibility nomograph established by Wischmeier and Smith (1978). The nomograph produces K values based on

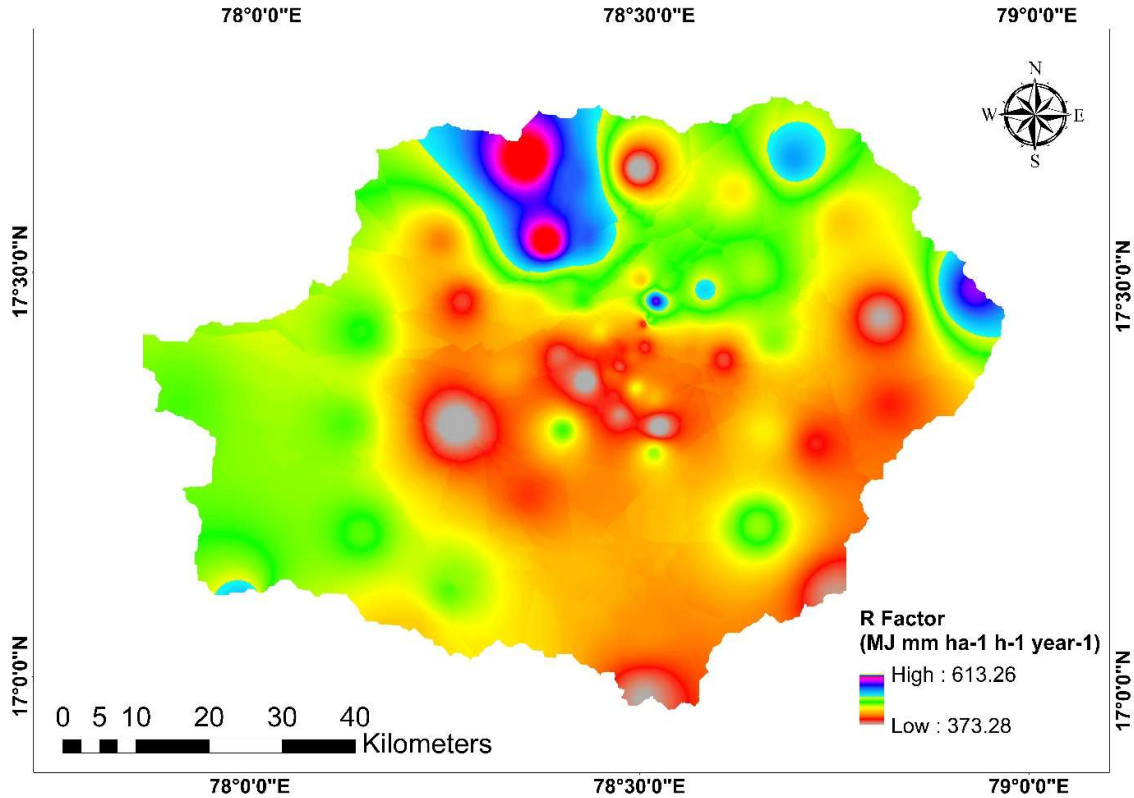

Fig. 3: R Factor Map of the study area.

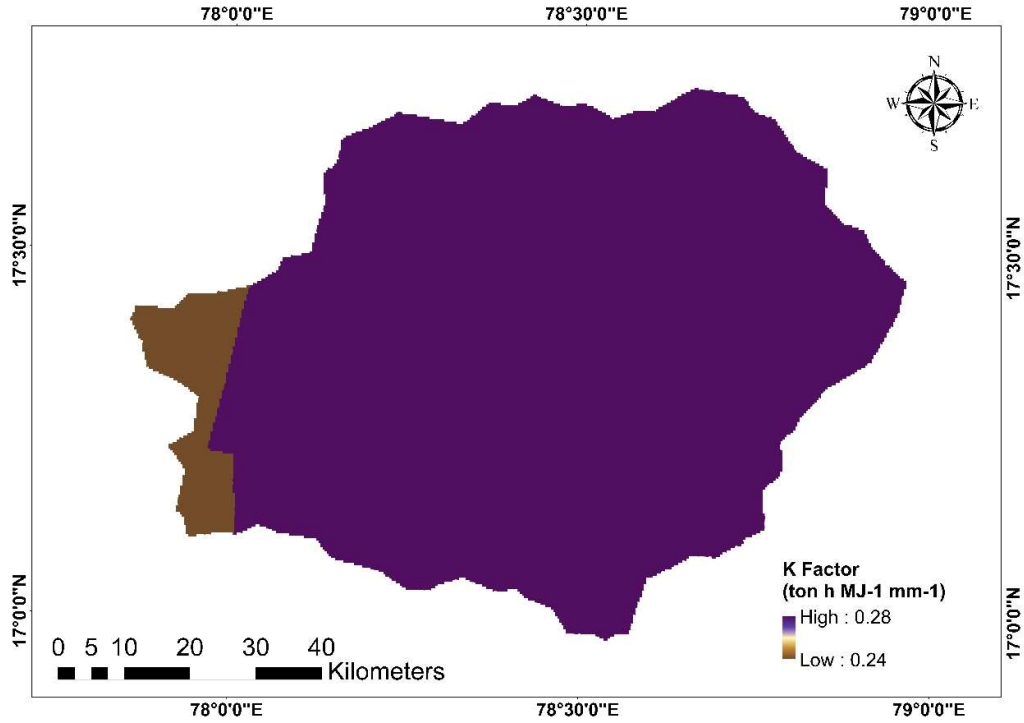

Fig.4: K Factor Map of the study area.

the percentages (%) of very fine sand, silt, organic matter (OM) content, structural code, and soil permeability code. In this research area, the major soil types are clay loam and clayey soils. Clay loam soils account for 94% of the area, while clay soils account for 6% of the research area. The K Factor map is depicted in Fig. 4. From Fig. 4, it is perceived that the soil erodibility in the research area ranges from 0.24 to 0.28 ton.h^{-1}.MJ^{-1}.mm^{-1}. The high plasticity of Silt and clay-based soils makes them less susceptible to soil erosion.

LS Factor

The LS factor, representing the combined effects of slope length (L) and slope steepness (S), plays a critical role in estimating soil erosion rates within the study area. The research area exhibits a diverse topography, with slopes ranging from 0 to 55 degrees and elevations varying between 330 and 770 meters above sea level. The LS factor values within the study area range from 0 to 118, reflecting variations in the potential for soil erosion driven by differences in slope gradient and flow accumulation. These values highlight regions prone to higher erosion risk due to steep slopes and concentrated water flow (Ganasri & Ramesh 2016). The study area's LS Factor spans from 0 to 118. Fig. 5 presents the LS factor map.

C Factor

C Factor values are determined based on the LULC Map. LULC map is created using Sentinel data and the CART algorithm in the Google Earth Engine platform by considering Agriculture, Vegetation, Waterbody, Built-up, and Barren Land as the classes (Li et al. 2021). Analysis reveals that the agriculture class is the dominant feature in the study area, accounting for 51.4% of the study area, followed by the Built-up class with 24.26% of the area. Barren Land, Waterbody, and Vegetation accounted for 20.48%, 2.6%, and 1.26% of the research area, respectively. The total accuracy of the LULC map is 89.6% and the kappa coefficient of 0.86 indicates the authenticity of the LULC map (He et al. 2020). LULC classification in Google Earth Engine and accuracy details are presented in Fig. 6. The LULC statistics are presented in Table 1. The C Factor

Table 1: LULC Statistics.

LULC	Area [Sq.km]	% of Area
Waterbody	164	2.6
Agriculture	3263	51.4
Vegetation	80	1.26
Built-up	1540	24.26
Barren Land	1300	20.48

value in the current research ranges from 0 to 1, 0 indicating no erosion risk and 1 representing significant erosion risk (Zhou et al. 2020). The C factor map is represented in Fig. 7.

P Factor

The P factor explains how surface runoff affects runoff concentration, runoff velocity, hydraulic forces, and drainage patterns, which in turn decrease the erosion amount that could occur from runoff. The P factor's value ranges from 0.2 to 4.5, with a value near 0.2 indicating good protection practices. However, the value near 4.5 indicates inadequate protection measures. The p Factor map is depicted in Fig. 8.

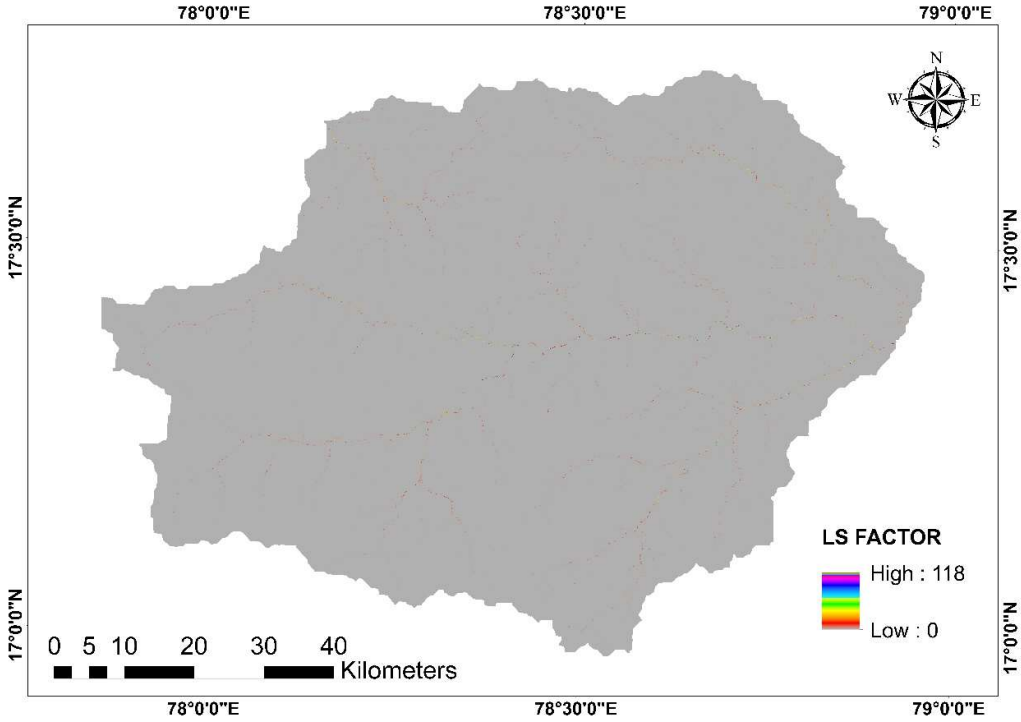

Fig. 5: LS Factor map of the Study area.

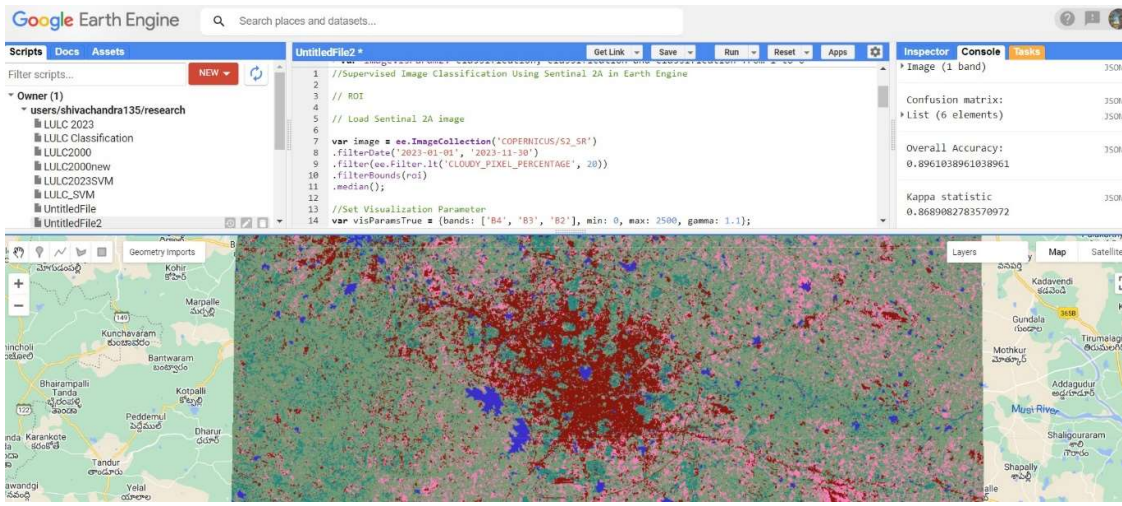

Fig. 6: LULC Classification in Google Earth Engine.

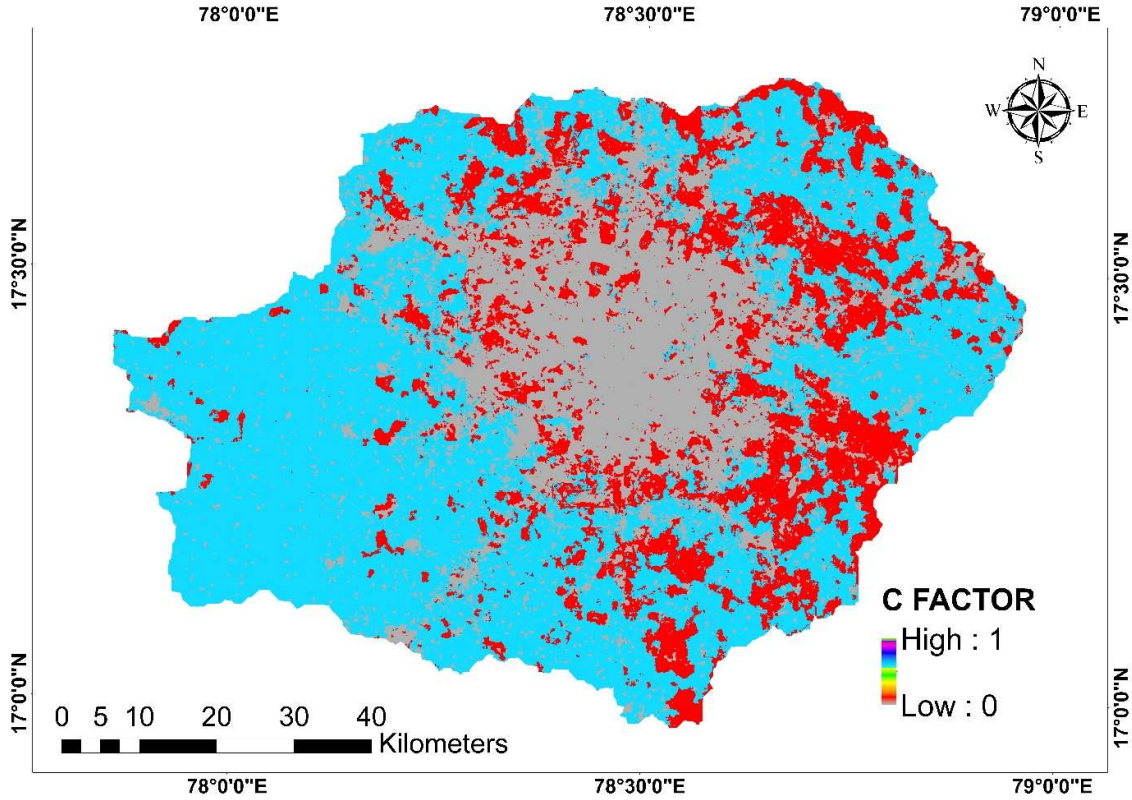

Fig. 7: C Factor Map of the Study Area.

Soil Erosion

Rainfall erosivity, steepness and length of slope, land cover management, soil erodibility, and soil conservation show the primary erosion contributors as per the RUSLE model. The spatial maps prepared by using the above-discussed procedures were converted to the same resolution using Resampling techniques in ArcMap 10.7. Then, by using the Raster calculator function in ArcMap 10.7, all the above maps have been multiplied to attain the final soil erosion map. According to Behera et al. (2020), the soil erosion map is classified into six categories. These categories are as follows: 0-1, 1-5, 5-10,10-20,20-50, and >50 ton.ha^{-1}.y^{-1}. Analysis of the soil erosion map reveals that 58.6% of the total area has zero soil erosion. 37% of the area has a soil erosion of more than zero and less than one ton.ha^{-1}.y^{-1}, 3.6% of the area is having a soil erosion of more than one and less than 5 ton.ha^{-1}.y^{-1}, and a very small portion of the research area is having a soil erosion of more than 5 ton.ha^{-1}.yr^{-1}. The soil erosion map is presented in Fig.9. The statistics related to soil erosion are presented in Table 2. Balasubramani et al. (2015) analyzed the semi-arid Andipatti Watershed of Tamil Nadu, India, and the results of the study indicate that the annual average soil loss within the watershed is about 6 ton.ha.$^{-1}$y^{-1}. Suryawanshi et al. (2021) analyzed the soil erosion potential of Madhya Pradesh using the USLE/RUSLE model and found that the areas under severe risk were 1.09% and 1.80%, and very severe risk areas were 1.57% and 1.83% as estimated by the USLE and RUSLE models, respectively. The average annual soil erosion for the entire state, as obtained from the USLE and RUSLE models, was 5.80 ton.ha^{-1}.y^{-1} and 6.64 ton.ha^{-1}.y^{-1}, respectively. Padala Raja Shekar and Aneesh Mathew (2024) analyzed the soil erosion potential of Munneru watershed of Telangana and concluded that the mean annual soil loss was calculated to be 14.06 ton.ha^{-1}.y^{-1}, indicating a high soil erosion risk. Tarate and Pravendra (2021) analyzed the Koyna River basin

Table 2: Soil Erosion Statistics.

Soil Erosion	Area [Sq.km]	% of Area
0	3720	58.61
< 1	2350	37.03
1-5	230	3.62
5-10	25	0.39
10-20	12	0.19
20-50	6	0.09
>50	4	0.06

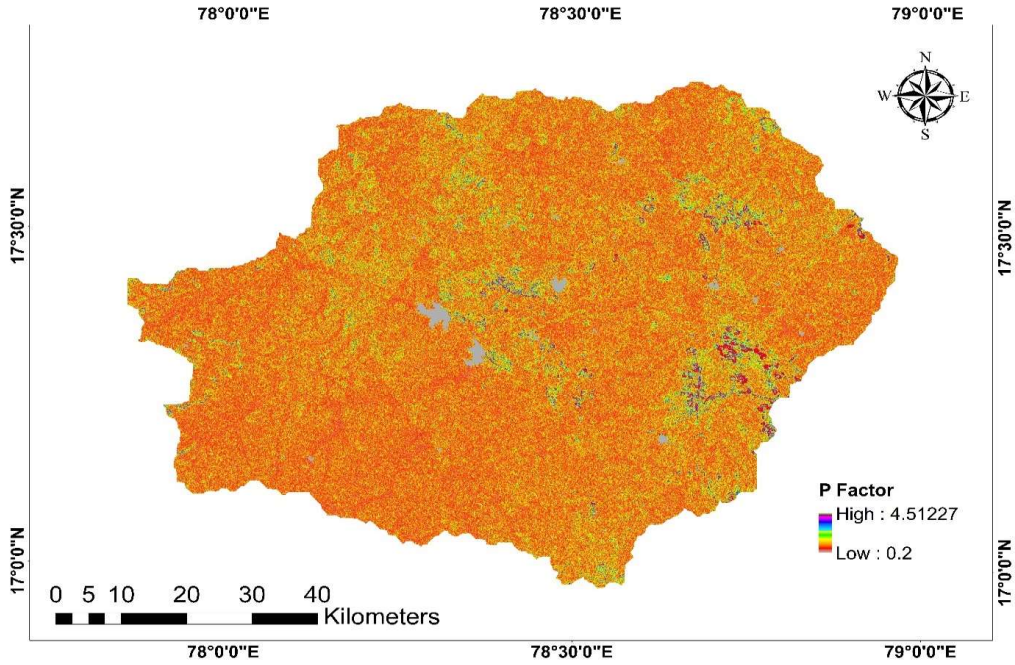

Fig. 8: P Factor Map of the Study Area.

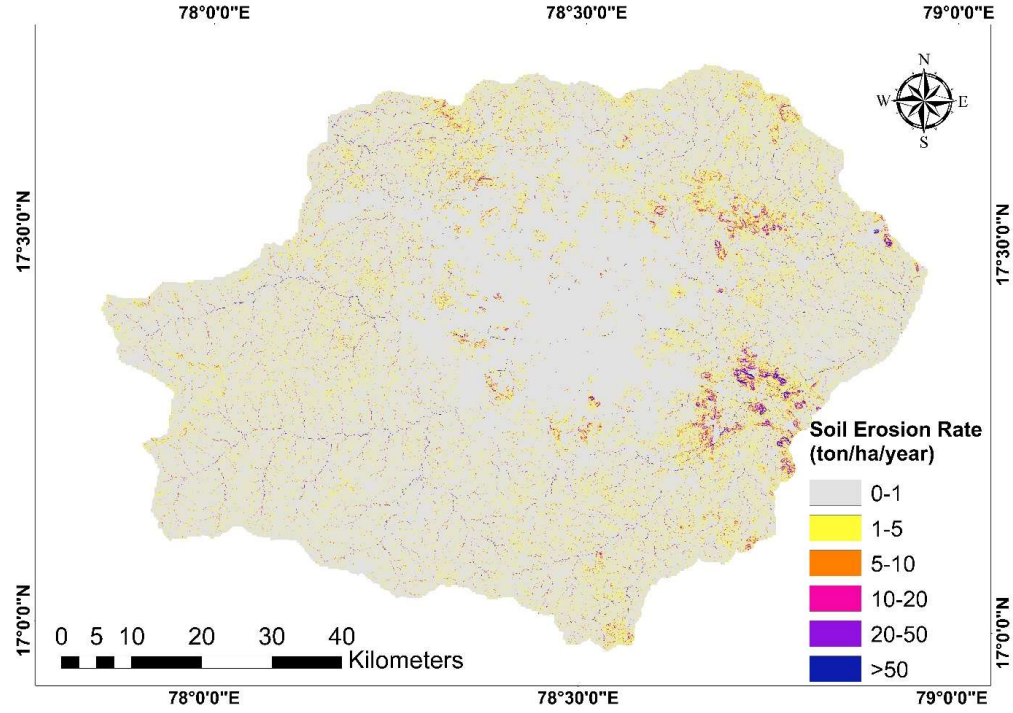

Fig. 9: Soil Erosion Map of the Study Area.

Table 3: Statistics of Sediment Yield.

Sediment Yield	Area [Sq.km]	% of Area
0-1	3864	60.88
1-7	1014	15.98
7-19	789	12.43
19-40	349	5.50
>40	331	5.22

for potential soil erosion and concluded that most of the study area has very low soil erosion risk.

Validation of RUSLE Model

Susceptible soil erosion data points for the year 2023, which corresponds to the land cover map year, were collected using Google Earth Pro. We then validated these sites using the ROC/AUC approach within the ArcGIS environment. The ROC-AUC was calculated using soil erosion sites by the ArcSDM function in ArcGIS software (Debnath et al. 2024). The ROC/AUC was divided into five categories: excellent (0.90–1.00), very good (0.80–0.90), good (0.70–0.80), average (0.60–0.70), and low (0.50–0.60). This classification provides a framework for understanding and assessing different levels of relationship quality (Owolabi et al. 2020). The RUSLE model has a good level of accuracy, measuring 72.8% (0.728).

Estimation of Sediment Yield

Sediment Yield is estimated using the RUSLE- Sediment Delivery Ratio model, and the Sediment yield map is classified into five classes. The statistics of sediment yield are shown in Table 3, and the sediment yield map is presented in Fig. 10. The analysis shows that 60.88% of the research area has a sediment yield of less than 1 ton.ha^{-1}.y^{-1}. 15.98% of the area accounts for a sediment yield of 1-7 ton.ha^{-1}.y^{-1}, 12.43% of the area accounts for a sediment yield of 7-19 ton.ha^{-1}.y^{-1}, and 10.72% of the study area accounts for more than 19 ton.ha^{-1}.y^{-1} of sediment yield. However, as urbanization tends to worsen soil erosion and sediment yield, it poses serious problems to water quality and environmental sustainability. Cities may offset these negative effects and build more resilient ecosystems by implementing sustainable land management strategies such as green infrastructure, stormwater management, and erosion control.

CONCLUSIONS

In conclusion, the RUSLE model has proven to be a strong and useful tool for estimating soil erosion when combined with Geographic Information System (GIS) technology. The importance of using cutting-edge computational tools and spatial analysis techniques to evaluate the intricate relationships between different factors influencing soil loss has been brought to light by this research. The accuracy and dependability of erosion predictions have increased due to the capacity to model erosion susceptibility at a finer spatial resolution and consider several contributing factors. The evaluation shows that more than 90% of the research area is

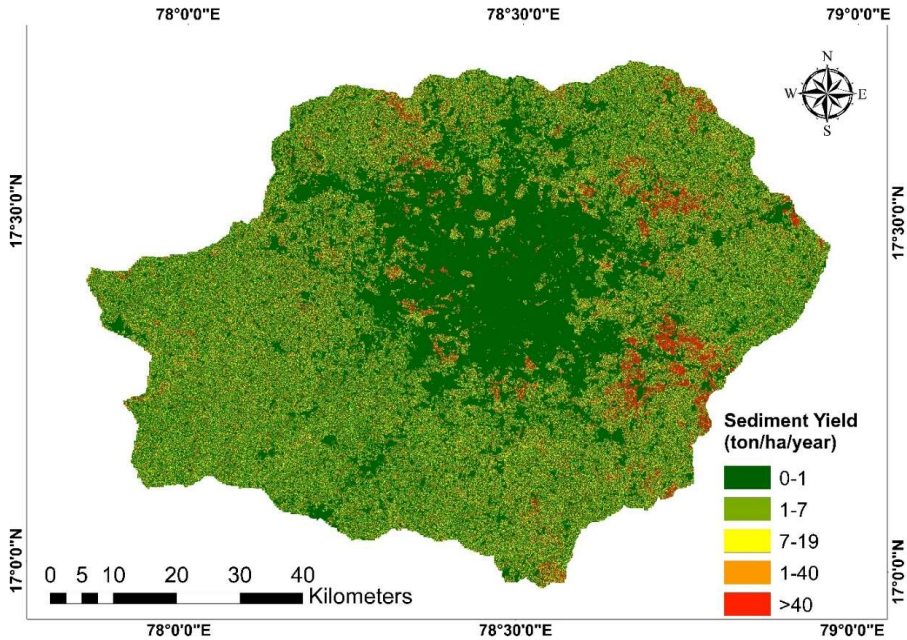

Fig. 10: Sediment Yield Map of the Study Area.

less prone to soil erosion and sediment yield, which is a good indication of preserving better soil for the future. In order to address today's environmental challenges, interdisciplinary approaches combining earth sciences, remote sensing, and computational modeling are essential. This research adds to the growing body on soil conservation and sustainable land management. In the end, RUSLE and GIS integration give land managers and decision-makers a useful toolkit to use proactive measures and protect our priceless soil resources for future generations.

REFERENCES

Abdo, H. and Salloum, J., 2017. Mapping the soil loss in Marqya Basin, Syria, using the RUSLE model in GIS and RS techniques. *Environmental Earth Sciences*, 76, p.114.

Allafta, H. and Opp, C. 2022. Soil erosion assessment using the RUSLE model, remote sensing, and GIS in the Shatt Al-Arab Basin (Iraq-Iran). *Applied Sciences*, 12(15), 7776. [DOI]

Amellah, O. and Morabiti, K., 2021. Assessment of soil erosion risk severity using GIS, remote sensing and RUSLE model in Oued Laou Basin (North Morocco). *Soil Science Annual*, 72, p.142530.

Ashiagbor, G., Forkuo, E.K., Laari, P. and Aabeyir, R., 2013. Modeling soil erosion using RUSLE and GIS tools. *International Journal of Remote Sensing and Geoscience*, 2(4), pp.1–17.

Bahadur, K., 2009. Mapping soil erosion susceptibility using remote sensing and GIS: A case of the Upper Namwa Watershed, Nan Province, Thailand. *Environmental Geology*, 57, pp.695–705.

Balasubramani, K., Veena, M., Kumaraswamy, K. et al., 2015. Estimation of soil erosion in a semi-arid watershed of Tamil Nadu (India) using the revised universal soil loss equation (RUSLE) model through GIS. *Modeling Earth Systems and Environment*, 1, p.10.

Behera, D.K., Saxena, M.R. and Ravi Shankar, G., 2017. Decadal landuse and landcover change dynamics in the east coast of India—Case study on Chilika Lake. *Indian Geographical Journal*, 93(1), pp.73–82.

Behera, M., Sena, D.R., Mandal, U., Kashyap, P.S. and Dash, S.S. 2020. Integrated GIS-based RUSLE approach for quantification of potential soil erosion under future climate change scenarios. *Environ. Monit. Assess.* 192, 733. [DOI]

Borrelli, P., Robinson, D.A., Panagos, P., Lugato, E., Yang, J.E., Alewell, C. and Ballabio, C., 2020. Land use and climate change impacts on global soil erosion by water (2015–2070). *Proceedings of the National Academy of Sciences*, 117(36), pp.21994–22001.

Dai, Q., Liu, Z., Shao, H. and Yang, Z., 2015. Karst bare slope soil erosion and soil quality: A simulation case study. *Solid Earth*, 6(3), pp.985–995.

Debnath, J., Debbarma, J., Debnath, A., Meraj, G., Chand, K., Singh, S.K. and Saikia, A., 2024. Flood susceptibility assessment of the Agartala urban watershed, India, using machine learning algorithm. *Environ. Monit. Assess.* 196 (2), 110.

Dutta, D., Das, S., Kundu, A. and Taj, A., 2015. Soil erosion risk assessment in Sanjal watershed, Jharkhand (India) using geo-informatics, RUSLE model and TRMM data. *Modeling Earth Systems and Environment*, 1, p.37.

Farhan, Y. and Nawaiseh, S., 2015. Spatial assessment of soil erosion risk using RUSLE and GIS techniques. *Environmental Earth Sciences*, 74, pp.4649–4669.

Fayas, C.M., Abeysingha, N.S., Nirmanee, S.K.G., Samaratunga, D. and Mallawatantri, A. 2019. Soil loss estimation using Rusle model to prioritize erosion control in KELANI River Basin in Sir Lanka. *Int. Soil Water Conserv. Res.* 7, 130–137.

Ganaie, T.A., Jamal, S. and Ahmad, W.S., 2020. Changing land use/land cover patterns and growing human population in the Wular catchment of the Kashmir Valley, India. *GeoJournal*, 86(4), pp.1–18.

Ganasri, B.P. and Ramesh, H., 2016. Assessment of soil erosion by RUSLE model using remote sensing and GIS—A case study of Nethravathi Basin. *Geoscience Frontiers*, 7, pp.953–961.

Gaonkar, V.G., Nadaf, F.M. and Kapale, V., 2024. Mapping and quantifying the integrated land degradation status of Goa using a geostatistical approach and remote sensing data. *Nature Environment & Pollution Technology*, 23(1). [DOI]

Gayen, A., Saha, S. and Pourghasemi, H.R., 2019. Soil erosion assessment using the RUSLE model and its validation by the FR probability model. *Geocarto International*, 35, pp.1750–1768.

He, Y., Li, Z. and Chen, J., 2020. Land use/land cover classification using remote sensing and machine learning algorithms: A review of recent advances and future prospects. *Remote Sensing*, 12(15), p.2358.

Jamal, S. and Ahmad, W.S., 2020. Assessing land use and land cover dynamics of wetland ecosystems using Landsat satellite data. *SN Applied Sciences*, 2(11), pp.1–24.

Jamal, S., Ahmad, W.S., Ajmal, U., Aaquib, M., Ali, M.A., Ali, M.B. and Ahmed, S., 2022a. An integrated approach for determining the anthropogenic stress responsible for the degradation of a Ramsar Site—Wular Lake in Kashmir, India. *Marine Geodesy*, pp.1–18. [DOI]

Kebede, Y.S., Endalamaw, N.T., Sinshaw, B.G. and Atinkut, H.B., 2021. Modeling soil erosion using RUSLE and GIS at the watershed level in the upper Beles, Ethiopia. *Environmental Challenges*, 2, p.100009.

Kolli, M.K., Opp, C. and Groll, M., 2021. Estimation of soil erosion and sediment yield concentration across the Kolleru Lake catchment using GIS. *Environ. Earth Sci.* 80, 161. [DOI]

Li, S., Liu, Y. and Wang, H., 2021. Land use and land cover change detection using Google Earth Engine. *ISPRS Journal of Photogrammetry and Remote Sensing*, 179, pp.112–122.

Liu, J. and Liu, H., 2020. Soil erosion changes during the last 30 years and contributions of gully erosion to sediment yield in a small catchment, southern China. *Geomorphology*, 368, p.107357.

Lu, D., Li, G., Valladares, G.S. and Batistella, M., 2004. Mapping soil erosion risk in Rondonia, Brazilian Amazonia: Using RUSLE, remote sensing and GIS. *Land Degradation and Development*, 15, pp.499–512.

Lufafa, A., Tenywa, M.M., Isabirye, M. and Majaliwa, M.J.G., 2003. Prediction of soil erosion in a Lake Victoria basin catchment using GIS-based Universal Soil Loss model. *Agricultural Systems*, 76, pp.883–894.

Maqsoom, A., Aslam, B., Hassan, U., Kazmi, Z. A., Sodangi, M., Tufail, R. F. and Farooq, D. 2020. Geospatial assessment of soil erosion intensity and sediment yield using the revised universal soil loss equation (RUSLE) model. *ISPRS International Journal of Geo-Information*, *9*(6), 356. [DOI]

McCool, D.C., Foster, G.R., Renard, K.G., Yoder, D.C. and Weesies, G.A., 1995. The revised universal soil loss equation. Department of Defense/ Interagency Workshop on Technologies to Address Soil Erosion on Department of Defense Lands San Antonio, TX, June 11–15.

McPhee, P.J. and Smithen, A.A., 1984. Application of the USLE in the Republic of South Africa. *Agricultural Engineering South Africa*, 18, pp.5–13.

Mesfln, A., 1994. The Nile—Source of regional cooperation or conflict. In: *Proceedings of the Eighth IWRA World Congress on Water Resources Satisfying Future National And Global Water Demand*, Cairo, Egypt, 21–25 November.

Moore, I.D. and Burch, G.J. 1986. Physical basis of the length-slope factor in the universal soil loss equation. *Soil Sci. Soc. Am. J.*, 50, 1294–1298.

Opeyemi, O.A., Abidemi, F.H. and Victor, O.K., 2019. Assessing the impact of soil erosion on residential areas of Efon-Alaaye Ekiti, Ekiti State, Nigeria. *International Journal of Environmental Planning and Management*, 5(1), pp.23–31.

Owolabi, S.T., Madi, K., Kalumba, A.M. and Orimoloye, I.R. 2020. A groundwater potential zone mapping approach for semi-arid

environments using remote sensing (RS), geographic information system (GIS), and analytical hierarchical process (AHP) techniques: a case study of Buffalo catchment, Eastern Cape, South Africa. *Arab. J. Geosci.* 13, 1184. [DOI]

Pan, J. and Wen, Y., 2014. Estimation of soil erosion using RUSLE in Caijiamiao watershed, China. *Natural Hazards*, 71, pp.2187–2205.

Panagos, P., Borrelli, P., Meusburger, K., Yu, B., Klik, A., Lim, K.J. and Sadeghi, S.H., 2017. Global rainfall erosivity assessment based on high temporal resolution rainfall records. *Scientific Reports*, 7(1), pp.1–12.

Padala, R.S. and Mathew, A., 2024. GIS-based assessment of soil erosion and sediment yield using the revised universal soil loss equation (RUSLE) model in the Murredu Watershed, Telangana, India. *HydroResearch*, 7, pp.315–325.

Perovic, V., Zivotic, L., Kadovic, R., Dordevic, A., Jaramaz, D., Mrvic, V. and Todorovic, M., 2013. Spatial modelling of soil erosion potential in a mountainous watershed of south–eastern Serbia. *Environmental Earth Sciences*, 68, pp.115–128.

Poesen, J., Nachtergaele, J., Verstraeten, G. and Valentin, C., 2003. Gully erosion and environmental change: Importance and research needs. *Catena*, 50, pp.91–133.

Prasanna Kumar, V., Shiny, R., Geetha, N. and Vijith, H., 2011. Spatial prediction of soil erosion risk by remote sensing, GIS and RUSLE approach: A case study of Siruvani River watershed in Attapady Valley, Kerala, India. *Environmental Earth Sciences*, 64, pp.965–972.

Prosdocimi, M., Cerdà, A. and Tarolli, P., 2016. Soil water erosion on Mediterranean vineyards: A review. *Catena*, 141, pp.1–21.

Qin, S., Liu, Z., Qiu, R., Luo, Y., Wu, J., Zhang, B., Wu, L. and Agathokleous, E., 2023. Short–term global solar radiation forecasting based on an improved method for sunshine duration prediction and public weather forecasts. *Applied Energy*, 343, p.121205.

Renard, K., Foster, G.R., Wessies, G.A. and Porter, J.P., 1994. RUSLE-revised universal soil loss equation. *Journal of Soil and Water Conservation*, 46, pp.30–33.

Renard, K.G., Foster, G.R., Weesies, G.A., McCool, D.K. and Yoder, D.C., 1997. *Predicting Soil Erosion by Water: A Guide to Conservation Planning with the Revised Universal Soil Loss Equation (RUSLE)*. USDA Agricultural Handbook No. 703. Washington, DC: U.S. Department of Agriculture.

Sahana, M., Rihan, M., Deb, S., Patel, P.P., Ahmad, W.S. and Imdad, K., 2020. Detecting the facets of anthropogenic interventions on the palaeochannels of Saraswati and Jamuna. In: *Anthropogeomorphology of Bhagirathi-Hooghly River System in India*. CRC Press, pp.469–489.

Salahalden, V.F., Shareef, M.A. and Al Nuaimy, Q.A.M., 2024. Assessment of deposited red clay soil in Kirkuk City using remote sensing data and GIS techniques. *Nature Environment & Pollution Technology*, 23(2). [DOI]

Schmidt, J., 2000. *Soil Erosion: Application of Physically Based Models*. Springer Science and Business Media.

Siswanto, S.Y. and Sule, M.I.S., 2019. The Impact of slope steepness and land use type on soil properties in Cirandu Sub-Sub Catchment, Citarum Watershed. In: IOP Conference Series: Earth and Environmental Science, International Seminar and Congress of Indonesian Soil Science Society 2019 5–7 August 2019, Bandung, West Java, Indonesia

Steinhoff-Knopp, B., Kuhn, T.K. and Burkhard, B., 2021. The impact of soil erosion on soil-related ecosystem services: Development and testing a scenario-based assessment approach. *Environmental Monitoring and Assessment*, 193(1), pp.1–18.

Stone, R.P. and Hilborn, D., 2000. *Fact Sheet: Universal Soil Loss Equation*. Ministry of Agriculture, Food and Rural Affairs, Guelph, ON, Canada, p.12.

Suryawanshi, A., Nema, A.K., Jaiswal, R., Jain, S. and Kumar Kar, S., 2021. Identification of soil erosion-prone areas of Madhya Pradesh using USLE/RUSLE. *Journal of Agricultural Engineering*, 58, pp.177–191. [DOI]

Swarnkar, S., Malini, A., Tripathi, S. and Sinha, R. 2018. Assessment of uncertainties in soil erosion and sediment yield estimates at ungauged basins: An application to the Garra River basin, India. *Hydrol. Earth Syst. Sci.* 22, 2471–2485.

Tarate, S. and Kumar, P., 2021. Geospatial technology for prioritization of the Koyna River Basin of India based on soil erosion rates using different approaches. *Environmental Science and Pollution Research*, 28, pp.1–24. [DOI]

Teng, M., Huang, C., Wang, P., Zeng, L., Zhou, Z., Xiao, W., Huang, Z. and Liu, C., 2019. Impacts of forest restoration on soil erosion in the Three Gorges Reservoir Area, China. *Science of the Total Environment*, 697, p.134164. [DOI]

Terranova, O., Antronico, L., Coscarelli, R. and Iaquinta, P., 2009. Soil erosion risk scenarios in the Mediterranean environment using RUSLE and GIS: An application model for Calabria (Southern Italy). *Geomorphology*, 112(3–4), pp.228–245.

Thomas, J., Joseph, S. and Thrivikramji, K.P., 2017. Assessment of soil erosion in a tropical mountain river basin of the southern Western Ghats, India, using RUSLE and GIS. *Geoscience Frontiers*, 9, pp.893–906.

Vanoni, V., 1975. Sedimentation engineering. Manuals and Reports on Engineering Practice. vol. 54. *American Society of Civil Engineers*

Wischmeier, W.H. and Smith, D.D., 1965. *Prediction Rainfall Erosion Losses from Cropland East of the Rocky Mountains: A Guide for Selection of Practices for Soil and Water Conservation*. USDA Agricultural Handbook No. 282. Washington, DC: U.S. Department of Agriculture.

Wischmeier, W.H. and Smith, D.D., 1978. *Predicting Rainfall Erosion Losses: A Guide to Conservation Planning*. USDA Handbook No. 537. Washington, DC: Department of Agriculture, Science and Education Administration.

Yesuph, A.Y. and Dagnew, A.B. 2019. Soil erosion mapping and severity analysis based on Rusle model and local perception in the Beshillo Catchment of the Blue Nile Basin, Ethiopia. *Environ. Syst. Res.* 8, 17.

Zarris, D., Vlastara, M. and Panagoulia, D., 2011. Sediment delivery assessment for a transboundary Mediterranean catchment: the example of Nestos River catchment. *Water Resources Management*. [DOI]

Zhao, G., Mu, X., Wen, Z., Wang, F. and Gao, P., 2013. Soil erosion, conservation, and eco-environment changes in the Loess Plateau of China. *Land Degradation and Development*, 24(5), pp.499–510.

Zhou, H., Yang, Z. and Zhang, Q., 2020. Estimating soil erosion risk in China based on the RUSLE model: A case study of the Loess Plateau. *Journal of Soil and Water Conservation*, 75(5), pp.619–628. [DOI]